Generation of pure bulk valley current in graphene

Yongjin Jiang[1],* Tony Low[2], Kai Chang[3], Mikhail I. Katsnelson[4], and Francisco Guinea[5]
[1] *Department of Physics, ZheJiang Normal University, Zhejiang 321004, People's Republic of China*
[2] *IBM T.J. Watson Research Center, Yorktown Heights, NY 10598, USA*
[3] *SKLSM, Institute of Semiconductors, Chinese Academy of Sciences, P.O. Box 912, Beijing 100083, Peoples Republic of China*
[4] *Radboud University Nijmegen, Institute for Molecules and Materials, Heyendaalseweg 135, 6525AJ Nijmegen, The Netherlands*
[5] *Instituto de Ciencia de Materiales de Madrid. CSIC. Sor Juana Inés de la Cruz 3. 28049 Madrid, Spain*
(Dated: September 11, 2012)

The generation of valley current is a fundamental goal in graphene valleytronics but no practical ways of its realization are known yet. We propose a workable scheme for the generation of bulk valley current in a graphene mechanical resonator through adiabatic cyclic deformations of the strains and chemical potential in the suspended region. The accompanied strain gauge fields can break the spatial mirror symmetry of the problem within each of the two inequivalent valleys, leading to a finite valley current due to quantum pumping. An all-electrical measurement configuration is designed to detect the novel state with pure bulk valley currents.

PACS numbers: 72.80.Vp,85.85.+j,73.63.-b

Apart from pseudospin (chirality), charge carriers in graphene are also characterized by the valley index (sometimes called isospin) originated from the existence of two conical (Dirac) points per Brillouin zone[1]. A valley polarized state requires the absence of time reversal symmetry, as the two valleys are related by this symmetry.

Motivated by the growing field of spintronics[2], it was proposed that the manipulation with the valley index may open a new way to transmit information through graphene, and different manipulation schemes were proposed[3–10]. After initial enthusiastic attitude, interest in "valleytronics" declined somehow, as it was soon realized that a valley polarized current will be degraded by intervalley scattering induced by atomic scale disorder[1], making it difficult the maintenance of valley polarized states. In addition, a number of proposals were based on the spatial separation of valley currents at zigzag edges[3], which requires well-defined edge orientation and at the same time free of short-range scattering.

We present a new scheme to induce valley polarized currents in graphene which avoids some of the pitfalls of previous proposals. The breaking of time reversal symmetry is achieved by means of time dependent fields, instead of a magnetic field. The induction of valley polarization by *a.c.* fields has been proven[11] in MoS_2 where optical radiation was used in order to excite valley polarized charge carriers. As in this experiment, the scheme discussed below generates valley currents throughout the entire system. However, the *a.c.* driving force in our proposal is due to mechanical vibrations of a nanoelectrical-mechanical system (NEMS[12–15]), as illustrated in Fig.1a.

We employ a continuum-medium description of graphene with the Dirac Hamiltonian,

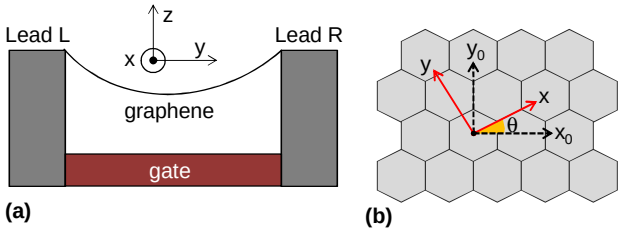

FIG. 1: Illustration and definitions of the **(a)** graphene based NEM device and **(b)** crystallographic coordinate systems used in the paper.

$$\mathcal{H}^{\pm}(\vec{k},\vec{\mathcal{A}}) = \hbar v_f[\pm(k_x \mp \mathcal{A}_x)\sigma_x + (k_y \mp \mathcal{A}_y)\sigma_y] + \mu \mathbb{1}_2, \quad (1)$$

where $+(-)$ denotes $K(K')$ valley index, v_f is the Fermi velocity and μ is the chemical potential. $\vec{\mathcal{A}}(\vec{r})$ is an effective gauge field describing the modifications to the hopping amplitudes induced by the strain fields $u_{ij}(\vec{r})$ [16, 17], and has opposite signs at the two valleys as required by time-reversal symmetry. We described the deformation of the suspended region, i.e. $-\frac{L}{2} < y < \frac{L}{2}$, with a simple uniaxial strain given by $u_{yy} = u$ and $u_{xx} = u_{xy} = 0$. It will be shown below that for arbitrary crystallographic orientation θ (see Fig.1b), $\vec{\mathcal{A}}(\vec{r})$ in the suspended region is given by the expression

$$\vec{\mathcal{A}}(\vec{r}) = \frac{\beta\kappa u}{a}(\text{-cos}3\theta, \sin 3\theta), \quad (2)$$

where $\beta \approx 2$ is the electron Gruneisen parameter and $\kappa \approx \frac{1}{3}$ is a parameter related to graphene's elastic property as described in [16]. $a \approx 1.4\mathring{A}$ is the interatomic distance. Adiabatic cyclic variations of the internal parameters, such as deformations in the strains (u) and

chemical potential (μ) in the suspended region, over a work cycle can constitute a scheme for adiabatic quantum pumping[18, 19] (for the general theory of quantum pumping, see Ref. [20, 21]). For the charge pumping one needs to break the inversion symmetry, e.g., making the right and left leads different (e.g., by different doping)[21]. Here we will demonstrate that for the case of *symmetric* leads the *valley* current through the system is, in general, nonzero. In this case, the pumping current through each channel will be shown to follow the general relation (with periodic boundary condition along the transversal x direction),

$$I^{pump,K}_{L/R}(k_x,\theta) = -I^{pump,K'}_{L/R}(-k_x,\theta), \tag{3}$$

where the subscript L/R refer to left/right leads($I_{L/R}$ is defined postive when the current flows out of the device). This significant relation results from an intrinsic symmety of graphene NEMs, as we will show later. Eq.(3) represents the central result of our paper. Below, we present the derivations leading to Eq.(3) and discuss the physical consequences that follows, such as the generation of pure bulk valley current and its possible experimental detection.

We start by considering the case $\theta = 0$, where the trench is directed along the zigzag direction (see the (x_0, y_0) coordinate system shown in Fig.1b). In this case, the Hamiltonian has the form of Eq.(1) and the pseudo-magnetic vector potential reads:

$$\begin{aligned} \mathcal{A}_x &= \frac{\beta\kappa}{a}(u_{xx}-u_{yy}), \\ \mathcal{A}_y &= -\frac{2\beta\kappa}{a}u_{xy}. \end{aligned} \tag{4}$$

For arbitrary orientation i.e. $\theta \neq 0$, Eq.(1) and Eq.(4) have to be recasted in the new coordinate frame (x, y). The two coordinate system are related by

$$\begin{pmatrix} x \\ y \end{pmatrix} = \mathcal{R}\begin{pmatrix} x_0 \\ y_0 \end{pmatrix} \quad , \quad \mathcal{R} = \begin{pmatrix} \cos\theta & \sin\theta \\ -\sin\theta & \cos\theta \end{pmatrix}. \tag{5}$$

The wave vector $\vec{k}$ transforms in the same way as $\vec{r}$ such that $\vec{k}\cdot\vec{r}$ is a rotational invariant quantity. The strain field is defined as, $u_{ij} = \frac{1}{2}(\frac{\partial u_j}{\partial x_i} + \frac{\partial u_i}{\partial x_j})$, which is a symmetric tensor of rank two. Hereafter we use the subscript/superscript "0" to denote physical quantities in the original frame (x_0, y_0). Thus, we have $\vec{k}_0 = R^{-1}\vec{k}$ and

$$\begin{aligned} u^0_{xx} - u^0_{yy} &= \cos 2\theta(u_{xx}-u_{yy}) - 2\sin 2\theta u_{xy}, \\ u^0_{xy} &= \frac{1}{2}\sin 2\theta(u_{xx}-u_{yy}) + \cos 2\theta u_{xy}. \end{aligned} \tag{6}$$

By using the new coordinates in the Dirac Hamiltonian, we can transform it to the rotated frame:

$$\mathcal{H}^{\pm}(\vec{k},\vec{\mathcal{A}}) = \hbar v_f \begin{pmatrix} \mu/\hbar v_f & e^{\mp i\theta}[(\pm k_x - ik_y) \mp (\pm\mathcal{A}_x - i\mathcal{A}_y)] \\ e^{\pm i\theta}[(\pm k_x + ik_y) \mp (\pm\mathcal{A}_x + i\mathcal{A}_y)]) & \mu/\hbar v_f \end{pmatrix}, \tag{7}$$

where we have defined the pseudo-magnetic field $\vec{\mathcal{A}}$ in the rotated frame as[22]:

$$\begin{pmatrix} \mathcal{A}_x \\ \mathcal{A}_y \end{pmatrix} = \mathcal{R}(3\theta)\begin{pmatrix} \frac{\beta\kappa}{a}(u_{xx}-u_{yy}) \\ \frac{-2\beta\kappa}{a}u_{xy} \end{pmatrix}. \tag{8}$$

Eqs.(7) and (8) constitute the continuum-medium description of stained-graphene in an arbitrarily rotated frame. Here follows two comments about this general form. First, if we perform the gauge transformation of the wave function on B sublattice $\psi^{\pm K}_B \longrightarrow \psi^{\pm K}_B e^{\pm i\theta}$, the Dirac Hamiltonian can be made explicitly invariant (i.e. Eq.(1)) under rotation. Thus, we can simply drop the factor $e^{\pm i\theta}$ in Eq.(7) in subsequent discussion. Second, from the definition for pseudo-magnetic field, it is obvious that the form is of $2\pi/3$ periodic in θ, which reflects the trigonal symmetry of the underlying honeycomb lattice.

Next, we describe the quantum pumping problem based on graphene NEMs[19, 23]. As discussed above, the derived Hamiltonian given by Eq.(7) is physically equivalent to Eq.(1). Suppose that between $-\frac{L}{2} < y < \frac{L}{2}$, the system has uniaxial strain $u_{yy} = u$ and $u_{xx} = u_{xy} = 0$, hence, Eq.(8) is reduced to

$$(\mathcal{A}_x, \mathcal{A}_y)(\vec{r}) = \begin{cases} 0, & |y| > \frac{L}{2} \\ (\frac{\beta\kappa u}{a})(-\cos 3\theta, \sin 3\theta), & |y| \leq \frac{L}{2} \end{cases} \tag{9}$$

with the expression given in Eq.(2) for the suspended region. In the following, assuming a particular geometry (the width $W \gg L$), the x direction is treated as translationally invariant. From Eq.(7) and Eq.(9), one can easily see that

$$\mathcal{H}^{+}(k_x, k_y, \vec{\mathcal{A}}, \theta) = \mathcal{H}^{-}(-k_x, k_y, \vec{\mathcal{A}}, -\theta). \tag{10}$$

We can call such combined symmetry as the *crystalline-angle-combined mirror symmetry* in the continuum-medium model. It turns out that such combined symmetry has a significant consequence on the relation of

pumping currents in each valley, i.e., Eq.(3), as will be elaborated further.

Due to the mentioned symmetry, we may focus only on the K Dirac cone, whose Hamiltonian has the following form for the different regions (i.e., $i = L, R, G$ denotes $y < -\frac{L}{2}$, $y > \frac{L}{2}$, $|y| \leq \frac{L}{2}$, respectively):

$$\mathcal{H}_i^+(\vec{k}, \vec{\mathcal{A}}) = \hbar v_f \begin{pmatrix} \epsilon_i/\hbar v_f & (\tilde{k}_x - i\tilde{k}_y)_i \\ (\tilde{k}_x + i\tilde{k}_y)_i & \epsilon_i/\hbar v_f \end{pmatrix}, \quad (11)$$

where we have defined $(\tilde{k}_x, \tilde{k}_y)_i = (k_x - \mathcal{A}_x, k_y - \mathcal{A}_y)_i$. In this paper, we consider mainly the symmetric case $\epsilon_L = \epsilon_R \neq \epsilon_G$.

The eigenenergies and eigenstates of the Hamiltonian in Eq.(11) read

$$\begin{aligned} E_i(\vec{k}) &= \epsilon_i + s\hbar v_f \sqrt{\tilde{k}_x^2 + \tilde{k}_y^2}, \\ \psi_i(\vec{k}) &= e^{i(k_x x + k_{y_i} y)} \begin{pmatrix} 1 \\ \frac{\hbar v_f (\tilde{k}_x + i\tilde{k}_y)_i}{E_s - \epsilon_i} \end{pmatrix}, \end{aligned} \quad (12)$$

where $s = \pm 1$ refers to electron/hole band, respectively. Due to translational invariance in x direction, k_x is the same in all three regions. We consider now the equilibrium situation where all three regions can be described by a common chemical potential μ. Obviously, $\tilde{k}_{x_i}$ is always real since k_x is real. Then, $\tilde{k}_{y_i} = \pm\sqrt{k_{f_i}^2 - \tilde{k}_{x_i}^2}$, where $k_{f_i} = \frac{\mu - \epsilon_i}{\hbar v_f}$ and the $\pm$ sign is selected to give the correct sign in the group velocity, depending whether it is an incident, transmitted, or reflected waves. Note that $\tilde{k}_y$ can be purely imaginary representing evanescent waves in the central region.

It is straightforward to calculate the scattering matrix for our device. Without loss of generality, we can focus on the case with the electron doping ($\mu - \epsilon_L > 0$) in the leads. The scattering coefficients are calculated to be

$$\begin{aligned} r_d &= e^{-ik_{y_L} L} \frac{C_2(d) + C_3(d)}{C_1(d)}, \\ t_d &= e^{-ik_{y_L} L} \frac{-4 \sin\varphi_L \sin\varphi_G e^{iA_y Ld}}{C_1(d)}, \end{aligned} \quad (13)$$

where r_d and t_d are the reflection and transmition coefficients with $d = 1(-1)$ corresponding to the cases with incident waves from $y = -\infty$ (left lead) and $y = \infty$ (right lead), respectively; φ_L and φ_G are defined through

$$e^{\pm i\varphi_L} = \frac{k_x \pm ik_{y_L} d}{k_{f_L}}, e^{\pm i\varphi_G} = \frac{\tilde{k}_{x_G} \pm i\tilde{k}_{y_G}}{k_{f_G}}. \quad (14)$$

The $C_i(d)$ in Eq.(13) are defined as

$$\begin{aligned} C_1(d) &= 4i \sin(\tilde{k}_{y_G} Ld)(1 - \cos\varphi_L \cos\varphi_G) \\ &- 4\cos(\tilde{k}_{y_G} Ld) \sin\varphi_L \sin\varphi_G, \\ C_2(d) &= -2i(1 + e^{2i\varphi_L}) \sin(\tilde{k}_{y_G} Ld), \\ C_3(d) &= 2ie^{i\varphi_L}[\sin(\tilde{k}_{y_G} Ld + \varphi_G) + \sin(\tilde{k}_{y_G} Ld - \varphi_G)]. \end{aligned} \quad (15)$$

Symmetries related with t_d and r_d. Next, we discuss symmetry properties of the scattering amplitudes. First, we note that $\varphi_G(d) = \varphi_G(-d)$, $\varphi_L(d) = -\varphi_L(-d)$ and they are independent of the sign of θ. Then, we can obtain the relations satisfied by C_i's: $C_1(d) = -C_1(-d)$, $C_{2,3}(-d)^* = C_{2,3}(d)$. Based on these relations and the odd parity of $\mathcal{A}_y(\theta)$, we arrive at:

$$\begin{aligned} t_d(k_x, \theta) &= t_{-d}(k_x, -\theta), \\ r_d(k_x, \theta) &= r_d(k_x, -\theta). \end{aligned} \quad (16)$$

Symmetry of pumped valley-dependent current. According to the adiabatic pumping theory[20] and the symmetry relations satisfied by r_d and t_d, we obtain the following relation for the pumping current $I_L^{pump,K}(k_x, \theta)$ for K valley:

$$\begin{aligned} & I_L^{pump,K}(k_x, \theta) - I_R^{pump,K}(k_x, -\theta) \\ &= \frac{ie\omega}{4\pi^2} \int_0^{2\pi/\omega} ds[\frac{dr_1(\theta)}{ds} r_1(\theta)^* - \frac{dr_{-1}(\theta)}{ds} r_{-1}(\theta)^*], \end{aligned} \quad (17)$$

where we've used s as time symbol to avoid confusion with transmission coefficient. Now, using the symmetry relations satisfied by C_i's and the fact that the common complex factors for C_2 and C_3, i.e., $ie^{i\varphi_L}$, is independent of time(see Eq.(19) for typical time dependence of pumping parameters for graphene NEM), we can simply prove that the integrand in Eq.(17) is zero. By further taking into account the current conservation condition($I_L^{pump,K}(k_x, -\theta) + I_R^{pump,K}(k_x, -\theta) = 0$) and the symmetry relation guaranteed by Eq.(10) (i.e., $I_L^{pump,K'}(-k_x, \theta) = I_L^{pump,K}(k_x, -\theta)$), we arrive at Eq.(3), the relation for pumped valley-dependent current, which is the central result of this paper.

Next, we discuss some direct consequences of Eq.(3). By integrating out the transversal wave vector k_x, we can get the following relation,

$$I_{L/R}^{pump,K}(\theta) = -I_{L/R}^{pump,K'}(\theta). \quad (18)$$

Eq.(18) means that the total pumping current at a given lead is opposite for different valleys. Thus, the total charge current is exactly zero. This situation is analogous to the pure spin current generation in spintronics[24, 25], thus we call this effect pure valley current generation. In summary, we have shown that the application of an alternating back gate voltage to graphene NEMs can induce a pure valley current via adiabatic pumping. In adiabatic pumping theory, there are two necessary conditions for finite charge pumping effect, i.e., time reversal symmetry breaking and mirror symmetry breaking of the the left/right leads[21]. The above derivations show that the valley pumping effect can be realized in a *seemingly* symmetric two-terminal geometry with identical leads. However, the mirror symmetry of the system (i.e. $y \to -y$) has actually been broken for each valley

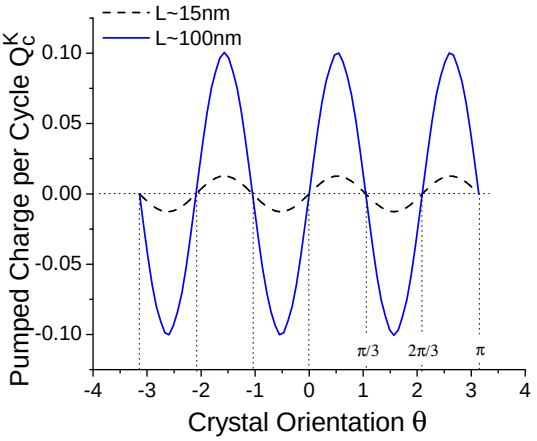

FIG. 2: (Color online) The pumped charge per cycle of the K valley, denoted as Q_c^K. The valley current can be obtained by $e\omega Q_c^K/2\pi$. The width is fixed to be $5000a$ ($\approx 700nm$), calculated for two different length as indicated. We fixed the phase difference of the driving parameters $\phi = \pi/2$ and take $|\vec{A}_{av}|/k_f \approx 0.002$, which amounts to a strain $u \approx 1.75 \times 10^{-4}$.

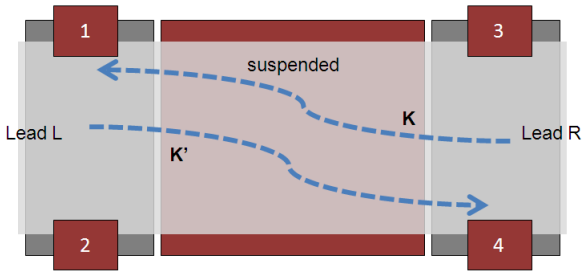

FIG. 3: (Color online) Pictorial sketch of the pumping generation of pure valley current and an all-electrical detection scheme. The Hall voltage difference $V_{12} = V_1 - V_2$ and $V_{34} = V_3 - V_4$ across the NEMs is predicted to bear opposite sign due to the flow of pure valley current.

when $\theta \neq \frac{n\pi}{3}$. Such symmetry breaking is embodied in the continuum theory through a nonzero $\mathcal{A}_y$ component. For comparison, we have $I_L^{pump,K/K'}(\theta = 0) = 0$ when $\mathcal{A}_y = 0$, which can be infered from the relation $I_L^{pump,K/K'}(k_x, \theta) = -I_L^{pump,K/K'}(k_x, -\theta)$ implicit in the discussion below Eq.(17). As is worthy to recapitulate, the symmetry property intrinsic to the graphene NEM(i.e., the *crystalline-angle-combined mirror symmetry*) can impose strong restriction of pumping currents on different valleys. For more quantitative understanding, we present some numerical results of $I_L^{pump,K}(\theta)$ (in terms of the pumped charge per cycle) for the K valley in Fig.2 using some typical experimental parameters, as discussed below.

As stated above, the strain (u) and Dirac potential (ϵ_G) in the suspended region are modulated by the ac back gate voltage. Near resonance, they differs by a phase difference ϕ with a typical time dependence given by(with conventional time symbol t)[19]:

$$\begin{aligned} \epsilon_G &= \epsilon_{G0}[1 + \delta\epsilon\cos(\omega t)]^{\frac{1}{2}}, \\ \vec{\mathcal{A}} &= \vec{\mathcal{A}}_0[1 + \delta\mathcal{A}\cos(\omega t + \phi)]^2. \end{aligned} \tag{19}$$

Assuming typical numbers for the static part $\epsilon_{G0} = \epsilon_L = 0.3eV$, $\vec{\mathcal{A}}_0 = 0.02k_f(\cos 3\theta, -\sin 3\theta)$, and the oscillating amplitude $\delta\epsilon = \delta\mathcal{A} = 0.2$, we calculated the pumped charge per cycle $Q_c^K(\theta)$ for K valley, as shown in Fig.2. By definition, the pumping current $I_L^{pump,K}(\theta) = e\omega Q_c^K(\theta)/2\pi$. Our calculation indicates a nearly linear scaling(unshown) of the pumping effect on length L of the NEMs, which is similar to results in[19]. As explicitly shown, the maximum pumping effect is reached for the crystallographic angles corresponding to armchair-type x axis ($\theta = \pi/2 + n\pi/3, n \in Z$) while it is zero at zigzag-type x axis ($\theta = n\pi/3, n \in Z$). The periodicity $2\pi/3$ with θ is easily seen. The valley current can be defined as $I^{pump,v}(\theta) = I^{pump,K}(\theta) - I^{pump,K'}(\theta)$, which is simply twice the value of $I^{pump,K}(\theta)$. For typical resonance frequency of $\omega \approx 10MHz$[14] to $0.16GHz$ [15], we arrive at numerical estimates $I^{pump,v} \approx 0.1 - 10\,\mathrm{pA}/\mu\mathrm{m}$, a quantity measurable in experiment.

The possibility of pure bulk valley current in this simple pumping scenario looks very promising. The problem is how to probe the valley current. Here we propose an all-electrical measurement as shown in Fig.3. From Eq.(3), we can infer that the charge current pertaining to carriers from the valley K not only has opposite longitudinal component with respect to the charge carriers from the valley K', but also their transversal velocities are opposite. As pictorially shown in Fig.3, we expect charges accumulating on opposite edges on the two sides of the NEMs. Based on this observation, we predict that the resultant Hall voltage on the left lead has opposite sign with that on the right lead, i.e., $\mathrm{Sign}(V_{12}/V_{34}) = -1$, which is the characteristic feature of the bulk valley current flow.

The above discussion can be made more clear if we consider the valley-dependent pumping Hall current, which can be calculated as $I_{L/R}^{Hall,K}(\theta) = \sum_{k_x} I_{L/R}^{pump,K}(k_x, \theta)\frac{k_x}{k_y}$. From Eq.(3) and the particle conservation law, we can obtain:

$$I_{L/R}^{Hall,K}(\theta) = I_{L/R}^{Hall,K'}(\theta) = -I_{R/L}^{Hall,K}(\theta). \tag{20}$$

Such Hall current on different leads can result in the opposite Hall voltage due to the charge accumulation near edges. Thus the existence of valley polarized currents possibly can be detected in the leads by means of nonlocal multiterminal measurements[26].

Our discussion above is restricted to the case with symmetrical leads. It is straightforward to extend our study to the more general case with differently doped leads. In the general situation, the current is not purely valley

current, i.e., $I_{L/R}^{pump,K}(\theta) \neq -I_{L/R}^{pump,K'}(\theta)$, thus the charge pumping current is finite. An example is again given by the case $\theta = 0$, where $I_{L/R}^{pump,K}(0) = I_{L/R}^{pump,K'}(0)$[19] and the valley current is zero.

To conclude, we have shown that through pumping induced by mechanical vibrations bulk valley polarized currents can be generated in graphene leads connecting the graphene resonator with trench directed at a general crystallographic angle. We have demonstrated that the generated current is purely valley current (with zero net charge pumping current) in the setup with the same doping rate in the graphene leads. Together with an all-electrical measurement scheme, our proposal opens a new direction of exploiting the valley degree of freedom, thus pushing forward graphene-based valleytronics a step forward toward real applications.

YJ and KC acknowledges the support from the National Natural Science Foundation of China (under grant No.11004174(YJ) and No. 10934007(KC)). TL also acknowledges partial support from NRI-INDEX. MIK acknowledges a financial support from FOM, The Netherlands. FG acknowledges financial support from Spanish MICINN(grantsFIS2008-00124, FIS2011-23713, CONSOLIDER CSD2007-00010), and ERC, grant 290846.

* jyj@zjnu.cn

[1] A. H. Castro Neto, F. Guinea, N. M. R. Peres, K. S. Novoselov and A. K. Geim, Rev. Mod. Phys. **81**, 109 (2009); N. M. R. Peres, Rev. Mod. Phys. **82**, 2673 (2010); S. Das Sarma, S. Adam, E. H. Hwang and E. Rossi, Rev. Mod. Phys. **83**, 407 (2011); M. I. Katsnelson, *Graphene: Carbon in Two Dimensions* (Cambridge Univ. Press, Cambridge, 2012).

[2] I. Zutic, J. Fabian, and S. Das Sarma, Rev. Mod. Phys. **76**, 323 (2004);

[3] A. Rycerz, J. Tworzydlo and C.W. J. Beenakker, Nature Phys. **3**, 172 (2007).

[4] I. Martin, Y. M. Blanter, and A. F. Morpurgo, Phys. Rev. Lett. **100**, 036804 (2011).

[5] J. M. Pereira, F. M. Peeters, R. N. Costa Filho and G. A. Farias, J. Phys. Condens. Matter **21**, 045301 (2009).

[6] Z. Wu, F. Zhai, F. M. Peeters, H. Q. Xu, and K. Chang, Phys. Rev. Lett. **106**, 176802 (2011).

[7] D. Xiao, W. Yao and Q. Niu, Phys. Rev. Lett. **99**, 236809 (2007).

[8] J. L. Garcia-Pomar, A. Cortija, and M. Nieto-Vesperinas, Phys. Rev. Lett. **100**, 236801 (2010).

[9] H. Schomerus, Phys. Rev. B **82**, 165409 (2010).

[10] T. Low and F. Guinea, Nano Lett. **10**, 3551 (2010).

[11] D. Xiao, G.-B. Liu, W. Feng, X. Xu, and W. Yang, Phys. Rev. Lett. **108**, 196802 (2012).

[12] J. S. Bunch, A. M. van der Zande, S. S. Verbridge, I. W. Frank, D. M. Tanenbaum, J. M. Parpia, H. G. Craighead and P. L. McEuen, Science **315**, 490 (2007).

[13] D. Garcia-Sanchez, A. M. van der Zande, B. L. A. San Paulo, P. L. McEuen and A. Bachtold, Nano Lett. **8**, 1399 (2008).

[14] C. Chen, S. Rosenblatt, K. I. Bolotin, W. Kalb, P. Kim, I. Kymissis, H. L. Stormer, T. F. Heinz and J. Hone, Nat. Nanotech. **4**, 861 (2009).

[15] A. Eichler, J. Moser, J. Chaste, M. Zdrojek, I. Wilson-Rae and A. Bachtold, Nat. Nanotech. **6**, 339 (2011).

[16] H. Suzuura and T. Ando, Phys. Rev B. **65**, 235412 (2002).

[17] M. A. H. Vozmediano, M. I. Katsnelson and F. Guinea, Phys. Rep. **496**, 109 (2010).

[18] E. Prada, P. San-Jose, and H. Schomerus, Phys. Rev. B **80**, 245414 (2009).

[19] T. Low, Y. Jiang, M. Katsnelson and F. Guinea, Nano Lett. **12**, 850 (2012).

[20] P. W. Brouwer, Phys. Rev. B **58**, R10135 (1998).

[21] M. Moskalets and M. Buttiker, Phy. Rev. B **66**, 205320 (2002).

[22] F. Zhai, X. Zhao, K. Chang, H. Q. Xu, Phys. Rev. B **82**, 115442 (2010).

[23] M. M. Fogler, F. Guinea and M. I. Katsnelson, Phys. Rev. Lett. **101**, 226804(2008).

[24] Koki Takanashi, Jpn. J. Appl. Phys.**49**, 110001 (2010).

[25] Y. Anishai, D. Cohen and N. Nagaosa, Phy. Rev. Lett. **104**, 196601 (2010).

[26] D. A. Abanin, S. V. Mozorov, L. A. Ponomarenko, A. S. Mayorov, M. I. Katsnelson, K. Watanabe, T. Taniguchi, K. S. Novoselov, and A. K. Geim, Science **332**, 6027 (2011).